



Microstructural Parameters of Hydroxypropylmethylcellulose Films Using X-ray Data

Puttanna Parameswara¹, Thippaiah Demappa², Tayur N Guru Row³, and Rudrappa Somashekar^{1*}

(1) Department of Studies in Physics, University of Mysore, Manasagangotri Mysore 570 006, India

(2) Department of Polymer Science, Sir MV, PG Center, University of Mysore Mandya-575 007, India

(3) Solid State and Structural Chemistry Unit, Indian Institute of Science Bangalore-560012, India

Received 13 May 2008; accepted 29 October 2008

ABSTRACT

The changes in microstructural parameters of edible polymer films of hydroxypropylmethylcellulose (HPMC) with plasticizers such as glycerol (GLY) and polyethylene glycol (PEG) have been studied using wide angle X-ray scattering (WAXS) data and line profile analysis (LPA). Exponential function for the column length distribution has been used for the determination of microstructural parameters. The crystal imperfection parameters such as crystal size $\langle N \rangle$, lattice strain $\%(g)$ and orientational parameters have been computed and correlated with the amount of plasticizers. Comparison of orientational parameter with increase in plasticizers suggests that there is increase in the orientation in HPMC films. The flexibility of the films is expected to increase due to decrease in the number of weak inter- and intramolecular hydrogen bonds with the addition of plasticizers. From these investigations it is also observed that there is increase in unit cell volume with increase in the plasticizers in HPMC films indicating greater stability of the blends which are essential in packing industry.

Key Words:

microstructure;
orientation;
particle size distribution;
strain;
WAXS.

INTRODUCTION

Hydroxypropylmethylcellulose (HPMC) is a polysaccharide, prepared from cellulose, with methyl and hydroxyl groups that render the cellulose molecule hydrophobic and hence it acquires surface-active properties. HPMC is water soluble, tasteless non-ionic derivative of cellulose, which has been accepted

as food additives in Europe, inactive ophthalmic preparations, oral capsules, suspension syrups, and eye drops [1-3]. Polysaccharide films have poor water vapour barrier properties because of their hydrophilic characteristic, but these hydrophilic polymers can form strong chain-to-chain inter-

(*) To whom correspondence to be addressed.
E-mail: rs@physics.uni-mysore.ac.in

action that provide a good barrier to O₂ and CO₂ [4,5]. A plasticizer molecule inserted into a polymer matrix and polymer-polymer bonds in matrix are replaced by weaker plasticizer-polymer bonds. The resulting increase in intermolecular spacing and weaker bonds allow the chains to slide when force is applied to the films [6,7]. Therefore the film is more flexible while the less dense structure is less resistant to force. The various studies were conducted in order to investigate correlation between hydration properties of HPMC and egg albumin (EA) matrices, gel microstructure and mobility, crystalline changes occurring in the gel and drug release [8].

HPMC, at room temperature, in solid phase is an entangled polymer network, with pockets of crystalline and amorphous regions. These regions play an important role in determining the physical properties of HPMC. We would like to relate some of these properties in terms of microstructural properties of HPMC with plasticizers (GLY, PEG). For this purpose we have developed a line profile analysis to quantify these crystalline regions using WAXS data and the results are correlated with the properties of HPMC. The reliability of the method used here has been established in the recently concluded IUCr round robin test [9].

EXPERIMENTAL

Materials and Methods

HPMC samples were supplied from Loba-Chem, Mumbai, India. Glycerol AR and polyethylene glycol 200-AR grade were obtained from S.D. Fine-Chem, Mumbai, India, and leveled glass plate (24 × 19 cm²) was used for preparation of the films.

Kinetic Measurements

Five gram of HPMC was dissolved in 100 mL of distilled water and stirred continuously. After being completely dissolved, HPMC solution was passed through 60 mesh sieve to remove undissolved (dust) particles. Then the solution was degassed to remove air bubbles and then solution was poured onto clean, dry and leveled glass plate, which was kept inside the oven. The temperature inside the chamber was maintained at 80 ± 5°C and dried for 1 h. Later the film was peeled off

from the glass plate and stored at room temperature and different concentrations with different plasticizers were used and various properties were studied.

X-Ray Diffraction Measurements

X-Ray powder pattern of HPMC samples were recorded using Philips PW 1140 diffractometer of Bragg-Brantoto Geometry (fine focus setting) with germanium monochromatic radiation of CuK_α (λ = 0.15420 nm) for 2θ range 5-50° at intervals of 0.003°, employing a curved position sensitive detector (CPSD) in the transmission mode. Figure 1 shows the XRD scans for all the samples.

LINE PROFILE ANALYSIS THEORY

Microstructural parameters such as crystal size (<N>) and lattice strain (%(g)) are usually determined by employing Fourier method of Warren and Averbach [10]. The intensity of a profile in the direction joining the origin to the centre of the reflection can be expanded in terms of Fourier cosine series;

$$I(s) = \sum_{n=-\infty}^{\infty} A(n) \cos\{2\pi nd(s-s_0)\} \quad (1)$$

where the coefficients of the harmonics, A(n), are functions of the size of crystallite and the disorder of the lattice. Here, s is sin(θ)/(λ), s₀ being the value of s at the peak of a profile, n is the harmonic order of coefficient, and d is the lattice spacing. The Fourier coefficients can be expressed as;

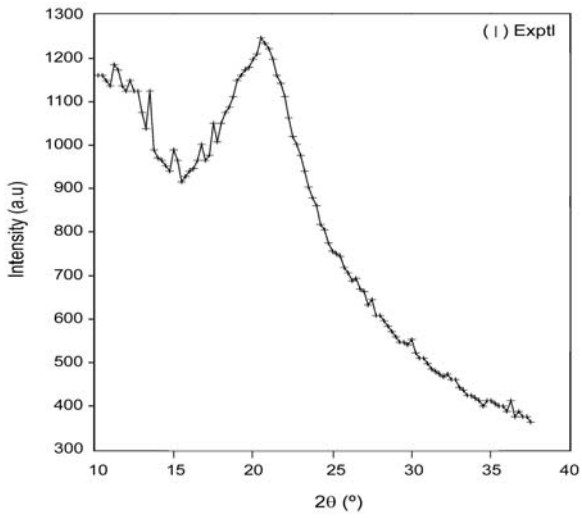
$$A(n) = A_s(n) \cdot A_d(n) \quad (2)$$

For a paracrystalline material, A_d(n) can be obtained with Gaussian strain distribution [11],

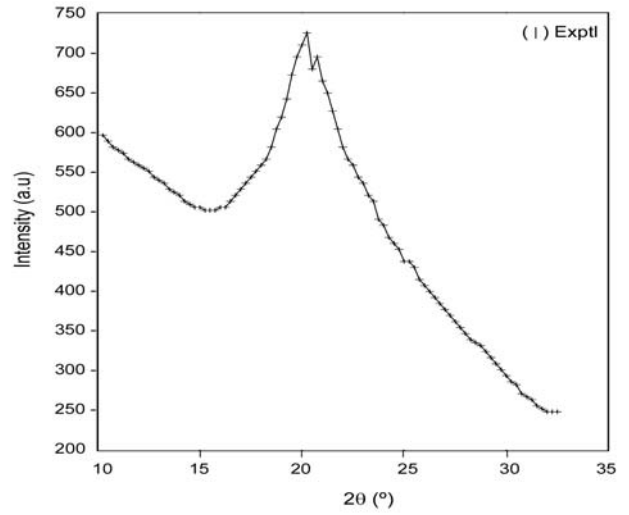
$$A_d(n) = \exp(-2\pi^2 m^2 n g^2) \quad (3)$$

Here, m is the order of the reflection and g = (Δd/d) is the lattice strain. Normally one also defines mean square strain <ε²>, which is given by g²/n. This mean square strain is dependent on 'n', whereas not on 'g' [12,13]. For a probability distribution of column lengths P(i), we have;

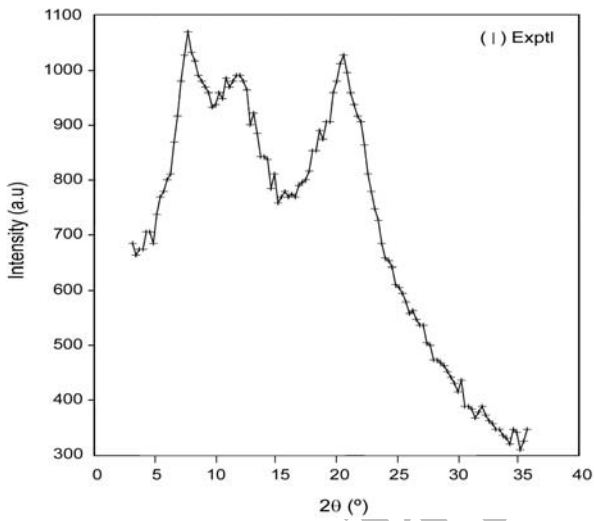
$$A_s(n) = 1 - \frac{nd}{D} - \frac{d}{D} \left[\int_0^n iP(n)di - n \int_0^n P(i)di \right] \quad (4)$$



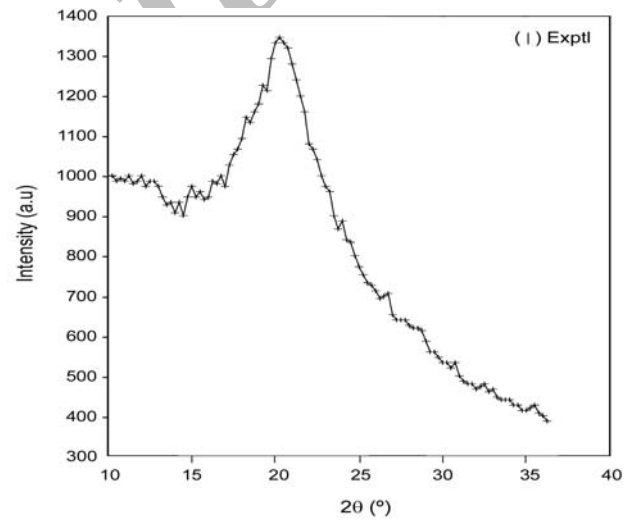
(a)



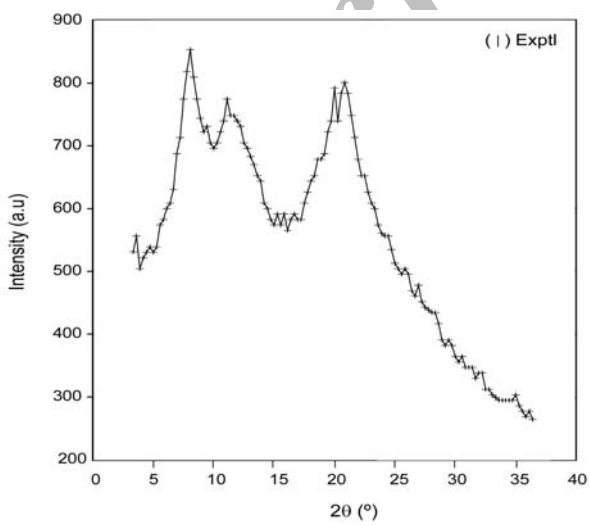
(d)



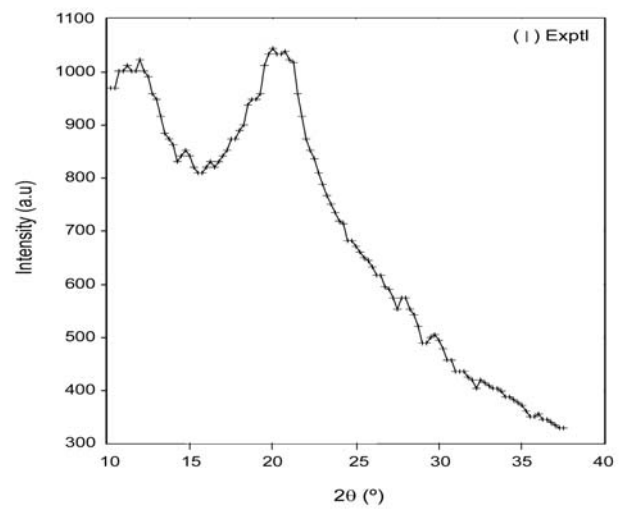
(b)



(e)



(c)



(f)

continued

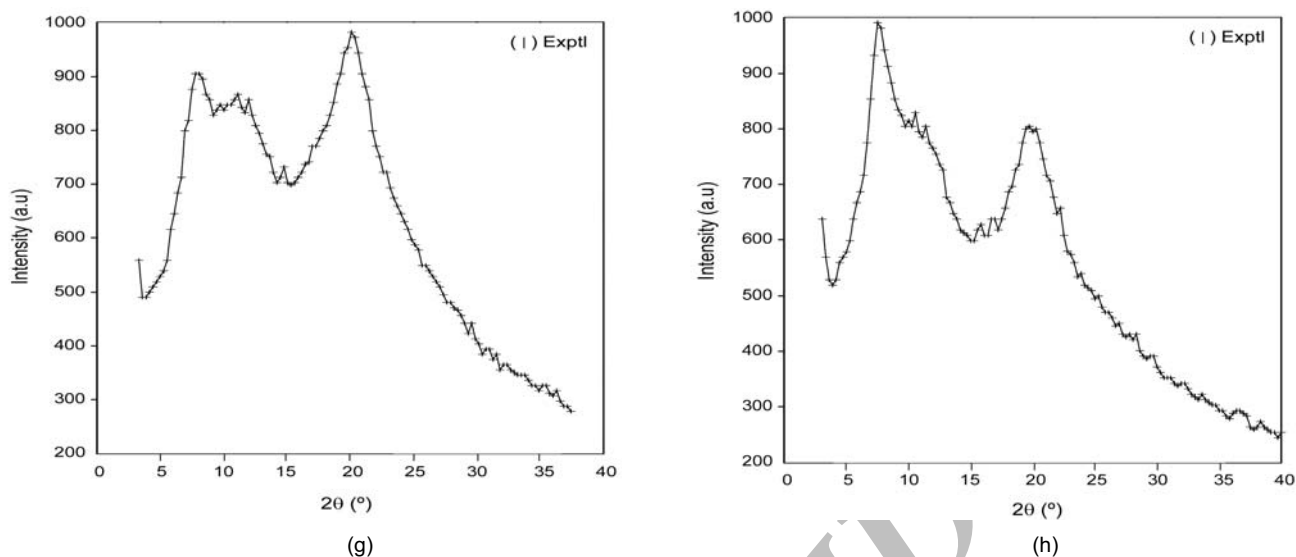


Figure 1. XRD scans of HPMC polymer samples with plasticizers. (a) HPMC, (b) 17% PEG in HPMC, (c) 37.5% PEG in HPMC, (d) 45% PEG in HPMC, (e) 17% GLY in HPMC, (f) 28.6% GLY in HPMC, (g) 37.5% GLY in HPMC, and (h) 45% GLY in HPMC.

where $D = \langle N \rangle d_{hkl}$ is the crystallite size and 'i' is the number of unit cells in a column. In the presence of two orders of reflections from the same set of Bragg planes, Warren [14] has shown a method of obtaining the crystal size ($\langle N \rangle$) and lattice strain (g in %). But in polymer it is very rare to find multiple reflections. So, to determine the finer details of microstructure, we approximate the size profile by simple analytical function for $P(i)$ by considering exponential functions. Another advantage of this method is that the distribution function differs along different directions. Whereas, a single size distribution function that is used for the whole pattern fitting, which we feel, may be inadequate to describe polymer diffraction patterns [13,15]. Here it is emphasized that the Fourier method of profile analysis (single order method used here) is quite reliable one as per the recent survey and results of round robin test conducted by IUCr [9]. In fact, for refinement, we have also considered the effect of background by introducing a parameter, for which ref 16 gives all the details on the effect of background on the microcrystalline parameters.

Exponential Distribution

It is assumed that there are no columns containing fewer than p unit cells and those with more decay exponentially. Thus, we have [17]:

$$P(i) = \begin{cases} 0 & ; \text{if } p < i \\ \alpha \exp\{-\alpha(i-p)\} & ; \text{if } p \geq i \end{cases} \quad (5)$$

where, $\alpha = 1 / (N - p)$. Substituting this in eqn (4), we obtain;

$$A_s(n) = \begin{cases} A(0)(1-n/\langle N \rangle) & ; \text{if } n \leq p \\ A(0)\{\exp[-\alpha(n-p)]\}/(\alpha N) & ; \text{if } n \geq p \end{cases} \quad (6)$$

Here, α is the width of the distribution function, 'i' is the number of unit cells in a column, n is the harmonic number, p is the smallest number of unit cells in a column, and $\langle N \rangle$ is the number of unit cells counted in a direction perpendicular to the (hkl) Bragg plane.

The procedure adopted for the computation of the parameters is as follows. Initial values of g and N were obtained using the method of Nandi et al. [18]. With these values in the equations the corresponding values for the width of distribution are obtained. These are only rough estimates, so the refinement procedure must be sufficiently robust to start with such values. Here we compute;

$$\Delta^2 = [I_{cal} - (I_{exp} + BG)]^2 / npt \quad (7)$$

where, BG represents the error in the background estimation, npt is number of data points in a profile, I_{cal} is intensity calculated using eqns (1) to (6) and I_{exp} is the experimental intensity. The values of Δ

Table 1. Microstructural parameters of HPMC with plasticizers (polyethylene glycol and glycerine) by using exponential distribution function.

Samples	2 θ (°)	g (%)	α	N	Δ	w	d ₁ /d ₂	ϵ_{lat}
HPMC	20.74	1.0 ± 0.02	0.78 ± 0.00	4.30 ± 0.11	0.026	1.41	1.79	0.443
17% PEG in HPMC	07.76	1.2 ± 0.05	1.36 ± 0.05	2.99 ± 0.12	0.041	0.97	2.55	0.437
	11.78	1.2 ± 0.06	2.61 ± 0.13	2.10 ± 0.10	0.050	1.45		
	20.60	1.0 ± 0.02	0.84 ± 0.02	4.15 ± 0.10	0.025	1.71		
37.5% PEG in HPMC	08.05	1.0 ± 0.04	1.09 ± 0.04	3.90 ± 0.14	0.036	0.68	2.58	0.450
	11.53	1.0 ± 0.05	2.32 ± 0.06	2.18 ± 0.05	0.026	1.33		
	20.56	1.0 ± 0.02	0.99 ± 0.02	3.96 ± 0.09	0.023	2.41		
45% PEG in HPMC	20.34	0.2 ± 0.00	0.83 ± 0.02	5.26 ± 0.11	0.022	1.65	1.98	0.101
17% GLY in HPMC	20.32	0.2 ± 0.00	0.67 ± 0.01	4.40 ± 0.12	0.028	1.63	1.65	0.066
28.6% GLY in HPMC	20.50	1.2 ± 0.03	0.90 ± 0.02	4.40 ± 0.10	0.024	1.38	1.72	0.032
37.5% GLY in HPMC	08.04	1.0 ± 0.03	1.62 ± 0.05	2.45 ± 0.08	0.033	0.79	2.59	0.494
	20.03	0.6 ± 0.01	0.92 ± 0.02	3.84 ± 0.09	0.024	2.70		
45% GLY in HPMC	07.65	0.8 ± 0.03	1.26 ± 0.05	2.25 ± 0.10	0.044	0.67	2.64	0.517
	20.00	0.2 ± 0.00	1.04 ± 0.02	3.86 ± 0.08	0.022	2.16		

were divided by half the maximum value of intensity so that it is expressed relative to the mean value of intensities, which are then minimized.

Computation of Microstructural Parameters

For the analysis, we have used X-ray diffraction data in the above equations to simulate the intensity profile by varying the necessary parameters until one obtains a good fit with the experimental profile. For this purpose, a multidimensional algorithm SIMPLEX is used for minimization [19]. We have used pure and plasticizers added HPMC polymer samples. The computed crystal imperfection parameters with reported physical parameters are given in Table 1 for exponential distribution function for each of the samples.

Orientation and Lateral Strain

Orientation of the HPMC crystallites was monitored using the azimuthal width 'w' of equatorial d₁ peak [20]. 'w' is related to the commonly used full-width at half-maximum by:

$$w = \frac{FWHM}{2\sqrt{\ln 2}} \quad (8)$$

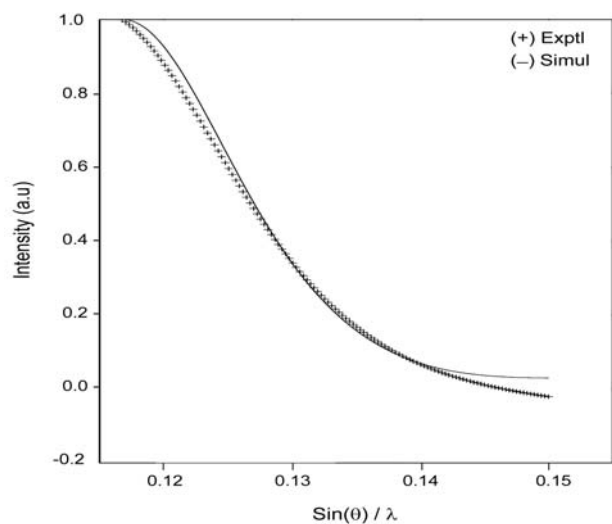
ϵ_{lat} is the lateral strain of HPMC defined as:

$$\epsilon_{lat} = -(d_1' - d_1) / d_1 \quad (9)$$

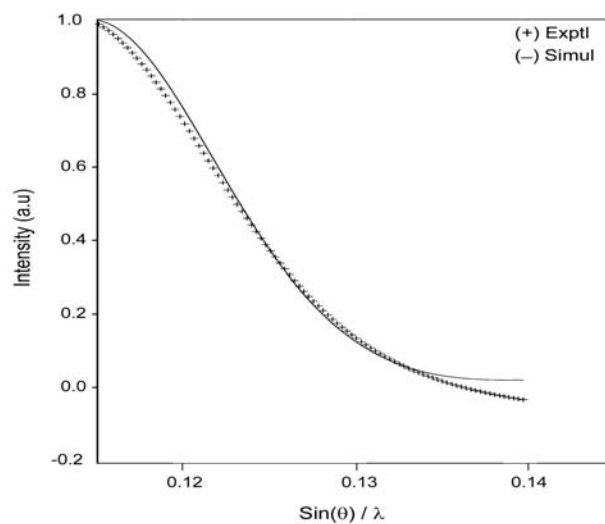
where d₁ and d₁' are unstressed and stressed d₁-spacing, respectively [21].

RESULTS AND DISCUSSION

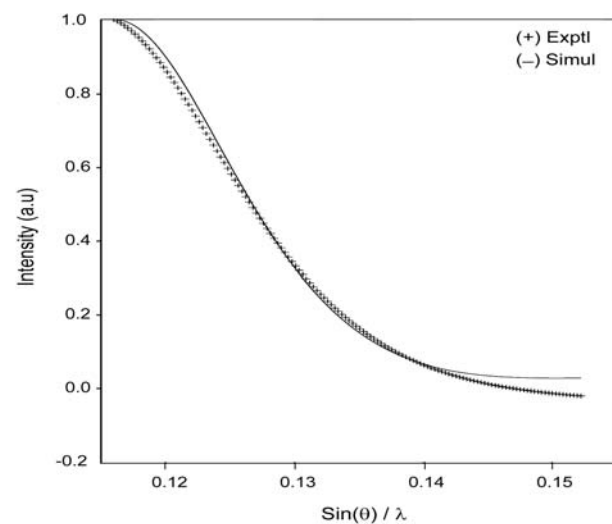
Figures 2a-2h show the credibility of the fit between simulated and experimental profiles of HPMC with and without plasticizers. Computed microstructural parameters are given in Table 1. It is evident from Figure 2 that there is a good agreement between simulated and experimental profiles with standard deviation being less than 5%. With addition of PEG and GLY in HPMC films we observe that the crystallite



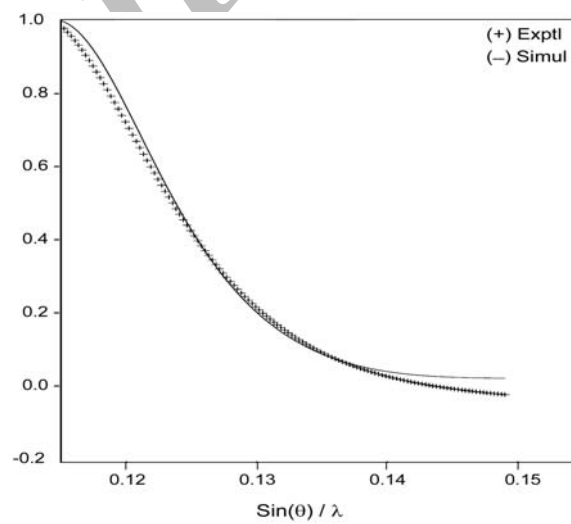
(a)



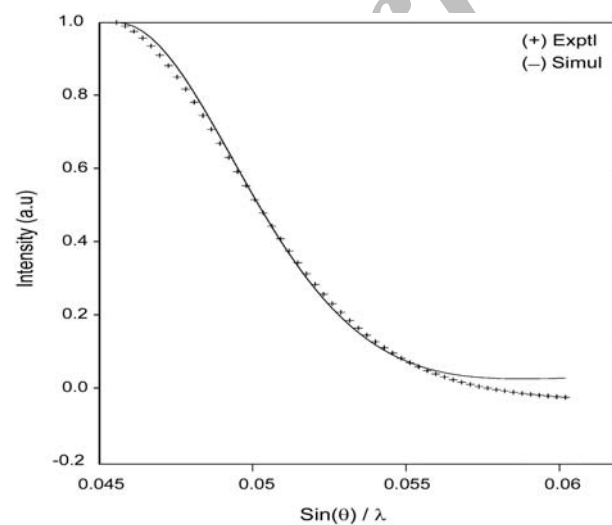
(d)



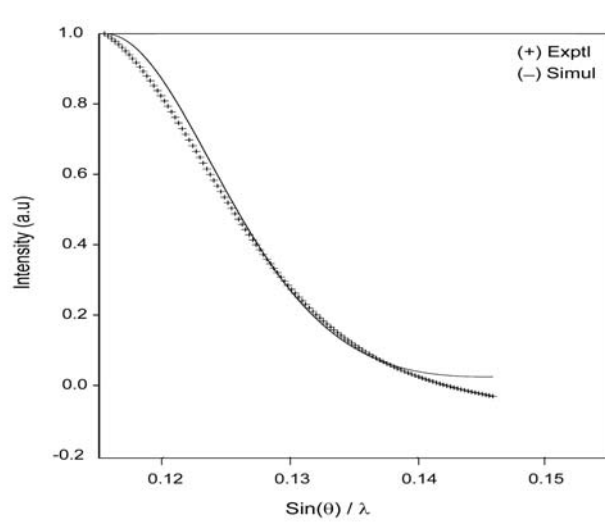
(b)



(e)



(c)



(f)

continued

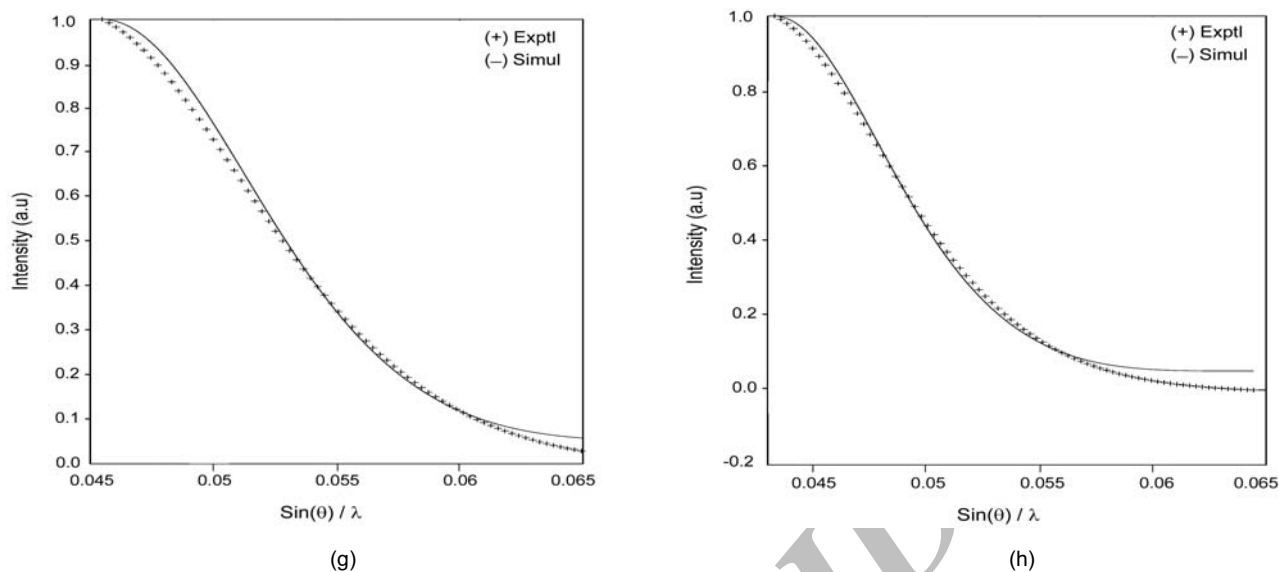


Figure 2. Experimental and simulated intensity profiles of X-ray reflection of HPMC polymer samples with plasticizers obtained with exponential column length distribution function. (a) HPMC, (b) 17% PEG in HPMC, (c) 37.5% PEG in HPMC, (d) 45% PEG in HPMC, (e) 17% GLY in HPMC, (f) 28.6% GLY in HPMC, (g) 37.5% GLY in HPMC, and (h) 45% GLY in HPMC.

size decreases. This indicates that the polymers networks presented in HPMC have reasonably higher crystallite size and shape which change with addition of plasticizers. HPMC without the presence of plasticizers is brittle in nature because of the presence of weak inter- and intramolecular hydrogen bonds. With the addition of plasticizers, the crystallite size is decreased. This implies essentially that there is a decrease in the number of weak hydrogen bonds. Indexing the observed reflections is difficult because of the limited number of reflections. Under these circumstances, we thought that a comparison of d_1 and d_2 , the lattice spacings of the first two reflections, which are commonly indexed as 110+200 and 200+310, respectively will give appropriate information on the changes in the unit cell. These values of the ratio d_1 and d_2 are given in Table 1. It is evident from Table 1 that d_1/d_2 increases with the addition of plasticizers, which essentially indicates that the unit cell volume also increases. Beyond 37.5% this decrease shows that there is a critical value associated with d_1/d_2 which is due to the critical number of formation of weak hydrogen bonds. However, the presence of a maximum in the values of d_1/d_2 was not observed in the case of GLY plasticizer. Further a comparison of full width at half maximum (FWHM)

computed from the well separated Bragg reflections using peak-fit method which is related to orientational parameter; do suggest that there is an increase in the orientation of the films with plasticizers in both cases. In the case of PEG plasticizer, there is a marked maximum value at 36% beyond which the orientation decreases. It is to be emphasized that these two aspects which are totally independent wherein in one case we look at the peak position and in another we look at the width of the profile. In this sense, two independent approaches have given a similar result. It is also observed that with addition of plasticizers, there is an inducement of the lateral strains in the sample and we have quantified this by calculating ϵ_{lat} given by eqn (9) using X-ray lattice spacing. An induced strain (ϵ_{lat}) also increases with increase in plasticizers. All these results justify the fact that with the addition of plasticizers, there is an increase in the amount of flexibility property of the HPMC films [22].

CONCLUSION

We have synthesized films of HPMC with addition of plasticizers like PEG and GEL using simple methods.

Further, we have quantified some of the changes in microcrystalline parameters, unit cell parameters, orientational parameters and induced lattice strains in these samples. These results indicate that with addition of plasticizers, there is a decrease in the number of weak inter- and intramolecular hydrogen bonds and hence an increase in the flexibility of the films which is essential in packing, coating and food industry. These changes in number of hydrogen bonds can be correlated by neutron scattering studies and IR recordings.

ACKNOWLEDGEMENTS

Authors thank Dr H Mirzadeh, Editor-in-chief of IPJ and the referees, for their suggestions to improve the presentation of this work.

REFERENCES

1. Wade A, Weller PJ, *Handbook of Pharmaceutical Percipients*, 2nd ed, 229-232, 1994.
2. Wang L, Xu Y, Graft copolymerization kinetics of ethyl acrylate onto hydroxypropyl methylcellulose using potassium persulphate as initiator in aqueous medium, *Iran Polym J*, **15**, 467-475, 2006.
3. Zhang JM, Gao JG, Sun XG, Peng Z, Diao J, Preparation and characterization of TiO₂/poly(St-co-MAA) core/shell composite particles, *Iran Polym J*, **16**, 39-46, 2007.
4. Ayranci E, Tunc S, Etcı A, The measurement of carbon dioxide transmission of edible films by a static method, *J Sci Food Agric*, **79**, 1033-1037, 1998.
5. Gaudin S, Lourdin D, Le Botlan D, Forsell P, Ilari JL, Colonna P, Effect of polymer-plasticizer interactions on the oxygen permeability of starch-sorbitol-water films, *Macromol Symp*, **138**, 245-248, 1999.
6. Siew DCW, Heilman C, Eastal AJ, Cooney RP, Solution and film properties of sodium cascinate/glycerol and sodium cascinate/polyethylene glycol edible systems, *J Agric Food Chem*, **47**, 3432-3440, 1999.
7. Mangavel C, Barbot J, Guéguen J, Popineau Y, Molecular determinants of the influence of hydrophilic plasticizers on the mechanical properties of cast wheat gluten films, *J Agric Food Chem*, **51**, 1447-1452, 2003.
8. Katzhendler I, Mäder K, Azoury R, Friedman M, Investigating the structure and properties of hydrated hydroxypropyl methylcellulose and egg album containing carbamazepine: EPR and NMR study, *Pharmac Res*, **17**, 1299-1308, 2000.
9. Balzar D, Report on the size-strain round robin, *IUCr Newsletter*, **228**, 14, 2002.
10. Sangappa, Demappa T, Mahadevaiah, Ganesha S, Divakara S, Manjunath Pattabi, Somashekar R, Physical and thermal properties of 8 MeV electron beam irradiated HPMC polymer films, *Nucl Inst Methods Phys Res B*, **266**, 3975-3980, 2008.
11. Hall IH, Somashekar R, The determination of crystal size and disorder from X-ray diffraction photograph of polymer fibres. 2. Modelling intensity profiles, *J Appl Cryst*, **24**, 1051-1059, 1991.
12. Ribarik R, Ungar T, Gubicza J, MW P-fit: a program for multiple whole-profiles fitting of diffraction profiles by ab initio theoretical functions, *J Appl Cryst*, **34**, 669-676, 2001.
13. Popa NC, Balzar D, An analytical approximation for a size broadened profile given by the lognormal and gamma distribution, *J Appl Cryst*, **35**, 338-346, 2002.
14. Warren BE, A generalized treatment of cold work in powder patterns, *Acta Cryst*, **8**, 483-486, 1955.
15. Scardi P, Leoni M, Diffraction line profiles from polydisperse crystalline systems, *Acta Cryst A*, **57**, 604-613, 2001.
16. Somashekar R, Hall IH, Carr PD, The determination of crystal size and disorder from X-ray diffraction photographs of polymer fibres. 1. The accuracy of determination of fourier coefficients of the intensity of a reflection, *J Appl Cryst*, **22**, 363-371, 1989.
17. Somashekar R, Somashekarappa H, X-Ray diffraction line broadening analysis: paracrystalline method, *J Appl Cryst*, **30**, 147-152, 1997.
18. Nandi RK, Kho HK, Schlosberg W, Wissler G, Cohen JB, Crist B Jr., Single-peak methods for Fourier analysis of peak shapes, *J Appl Cryst*, **17**,

- 22-26, 1984.
19. Press W, Flannery BP, Teukolsky S, Vetterling WT, *Numerical Recipes*, (Eds), Cmbridge University, 1986.
 20. Uchida T, Anderson DP, Minus M, Kumar S, Morphology and modulus of vapor grown carbon nano fibers, *J Matter Sci*, **41**, 5851-5856, 2006.
 21. Allen RA, Ward IM, Bashir Z, The variation of *d*-spacing with stress in the hexagonal polymorph of poly acrylonitrile, *Polymer*, **35**, 4035-4040, 1994.
 22. Ghanbarzadeh B, Oromiehie A, Musavi M, Rezayi R, Razmi E, Milani J, Investigation of water vapour permeability, hydrophobicity and morphology of zein films plasticized by polyols, *Iran Polym J*, **15**, 691-700, 2006.

Archive of SID